

Neutron Scattering of Novel Functional Magnetic Materials

A. K. Bera, A. Jain, A. Kumar, and S. M. Yusuf*

Solid State physics Division, Bhabha Atomic Research Centre, Mumbai 400085

Abstract

Advanced magnetic materials with improved functional magnetic properties are required for advances in technology and engineering. Microscopic understanding of the intertwined relation between the functionalities and structures (crystal/magnetic) of several functional magnetic materials is achieved by employing powerful neutron scattering technique. A glimpse of our recent results on some selective functional magnetic materials is presented here.

Keywords: Neutron scattering, antiferromagnets, spin chains, rare-earth manganites

Introduction

Novel functional magnetic materials are a group of material having interesting physical properties which are controlled/influenced by external applied magnetic field. These materials have applications in various fields ranging from data storage to medical investigations including drug delivery. Microscopic understanding of the relation between the structure (crystal/magnetic) and functionalities at the molecular and atomic scale is of paramount importance to advancing new technologies. The central point to achieve such microscopic understanding is the investigation of magnetic structure by neutron scattering [1]. In this article, we highlight recent developments in the study of functional magnetic materials in SSPD, BARC.

Investigation of low dimensional quantum magnets

Low-dimensional quantum magnets have received lots of attention in recent years as they represent tractable example of many body quantum systems. Low-dimensional magnetic systems refer to the system where the magnetic exchange interaction in one (two) directions is much higher compared with the values in the remaining two (one) directions. The reduction of dimensionality and small value of spin strongly enhance the quantum fluctuations in these compounds and lead to a range of exotic magnetic

phenomena. We have investigated such quantum phenomena in several naturally grown one- and two-dimensional magnetic materials [2-13].

Neutron scattering investigations of exotic quantum phases in a spin-1/2 metal-organic kagome compound

Among all geometrically frustrated networks, the $S = \frac{1}{2}$ nearest-neighbour Heisenberg antiferromagnet on the kagome lattice is a promising system where one can look for the novel quantum phenomena including the “resonating valence bond” state [14], gapped and gapless spin liquids as proposed theoretically for these systems. However, the experimental investigation of these systems is not easy because most of the kagome lattice antiferromagnets (AFMs) have either a large spin or a structural distortion. In our effort to investigate spin $\frac{1}{2}$ kagome lattice AFMs, we have synthesized a new compound with formula $\{[\text{Cu}_3(\text{CO}_3)_2(\text{bpe})_3] \cdot 2\text{ClO}_4\}_n$ (bpe=1,2-bis(4-pyridyl)ethane) [15], having ideal 2D kagome layers of Cu^{2+} ($3d^9$, $S=1/2$), in the crystallographic ab plane, with pillars of “bpe” ligands of length ~ 13.13 Å, separating the kagome layers [Fig. 1 (a)]. The $[\text{Cu}_3(\text{CO}_3)_2]^{2+}$ kagome layers in this compound are pillared by the bpe linkers along the c axis. The structural parameters for this compound make sure two-dimensionality of the kagome layers with a negligible inter-layer coupling.

The dc susceptibility [Fig. 1(b)] can be fit to a Curie-Weiss law at high temperatures ($T > 150$ K). The resulting Curie-Weiss temperature (θ_{CW}) of ~ -2.9 K implies an AFM exchange between the Cu^{2+} spins in the 2D kagome plane. In our neutron diffraction study [Fig. 1(c)], neither additional magnetic Bragg peaks nor an enhancement in the intensity of fundamental nuclear Bragg peaks has been observed down to 1.5 K, ruling out the presence of a long-range magnetic ordering (LRO). No depolarization of the neutron beam was observed down to 3 K, ruling out the presence of any ferromagnetic domains/clusters. Our Neutron diffraction and neutron depolarization measurements combined with the specific heat measurements [Fig. 1(b)] rule out the possibility of any LRO down to 86 mK. Our results suggest that strong quantum fluctuations enhanced by geometrical frustration suppress the long-range magnetic order and a spin-liquid like magnetic ground state is realized in this compound [2]. The derived phase diagram is shown in Fig.1 (d).

Magnetic correlations in the 2D honeycomb antiferromagnet $\text{Na}_2\text{Co}_2\text{TeO}_6$

In the quest for quantum spin liquids, the Kitaev honeycomb model is well known for its exact solvability and non-trivial properties that may be utilized in quantum computation. The model features bond-dependent **Ising interactions** (Kitaev interactions) between spin-1/2 degrees of freedom on a honeycomb lattice. Experimentally, the Kitaev honeycomb model has been realized only on 5d iridium and 4d ruthenium-based compounds [16,17]. Recently, it is proposed that the 3d Co^{2+} ions-based compounds can be also Kitaev materials [18]. Here, we report spin-spin correlations of the layered honeycomb compound $\text{Na}_2\text{Co}_2\text{TeO}_6$, a possible Kitaev material based on the 3d magnetic ion Co^{2+} . The magnetic layers consist of edge-

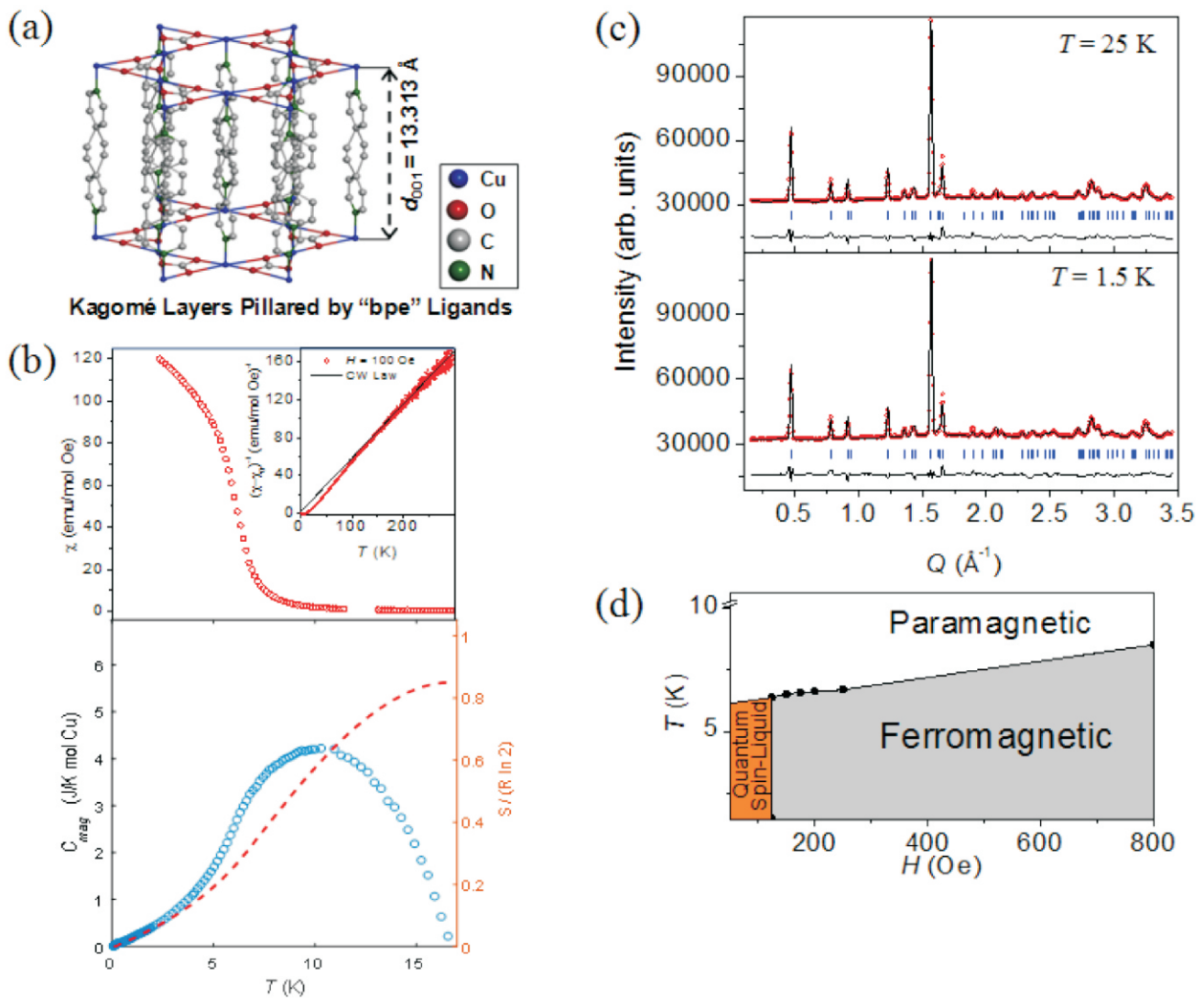


Fig. 1: (a) Crystal structure of the compound $\{[\text{Cu}_3(\text{CO}_3)_2(\text{bpe})_3]_2\text{ClO}_4\}_n$ (b) (top) temperature dependence of χ_{dc} measured with $H = 1000\text{e}$. Solid lines in the inset represent the Curie-Weiss (CW) fit. (bottom) Temperature dependence of the magnetic specific heat. The dashed line is the estimated magnetic entropy. (c) Observed (open circles) and calculated (solid lines) neutron diffraction patterns at 25 K and 1.5 K. (d) Magnetic phase diagram from neutron diffraction and thermodynamics measurements.

sharing CoO_6 and TeO_6 octahedra within the ab plane. The magnetic layers are well separated ($\sim 6 \text{ \AA}$) along the crystallographic c axis by the non-magnetic Na-layers providing a 2-dimensional magnetic system [Fig. 2]. The compound $\text{Na}_2\text{Co}_2\text{TeO}_6$ shows a zigzag AFM order below the $T_N = 25 \text{ K}$, due to the presence of an additional Heisenberg interaction (J) over the Kitaev interactions. The zigzag AFM state is proposed to be situated proximity to the quantum Kitaev spin-liquid state [3]. Our neutron powder diffraction study also reveals an anisotropic spin correlation in the ordered state, as evident from the different peak widths of the magnetic peaks $(000)+k$ and $(001)+k$ with $k = (0 \ 0 \ \frac{1}{2})$, with reduced order moments [Fig. 2]. Above the $T_N = 25 \text{ K}$, two-dimensional short-range spin-spin correlations have been found within the honeycomb planes [3].

Furthermore, our single crystal magnetization study reveals highly anisotropic magnetic behaviour and a suppression of the zigzag AFM order by an in-plane field of $\sim 6 \text{ T}$. Overall magnetic properties of $\text{Na}_2\text{Co}_2\text{TeO}_6$ manifest an intricate phase interplay that is generally expected near boundaries of competing phases, where quantum fluctuations are important.

Magnetic Hamiltonian of the spin-1 trimer chain compound $\text{CaNi}_3\text{P}_4\text{O}_{14}$

Low-dimensional magnetic materials, especially, one dimensional (1D) spin chains, are of current interest in condensed-matter physics as model experimental systems to study the physics of many-body quantum physics. Among them, the trimer spin chains are of particular interest due to the occurrence of

the magnetization plateaus, which can be viewed as an essentially macroscopic quantum phenomenon. At the magnetization plateau state magnetization is quantized to fractional values of the saturated magnetization value, analogous to the quantum Hall effect, proving a striking example of the macroscopic quantum phenomenon. We have investigated the spin-1 trimer chain compound $\text{CaNi}_3\text{P}_4\text{O}_{14}$ by elastic and inelastic neutron scattering. Experimental data reveal an AFM ordering below the $T_c = 16 \text{ K}$ and one-dimensional short-range spin correlations above the T_c [4]. Neutron inelastic data reveal gapped dispersive spin-wave excitations in the 3D long-range ordered magnetic state ($T_c = 16\text{K}$), and gapless magnetic excitations above the T_c due to the low-dimensional spin-spin correlations within chains [Fig. 3]. The

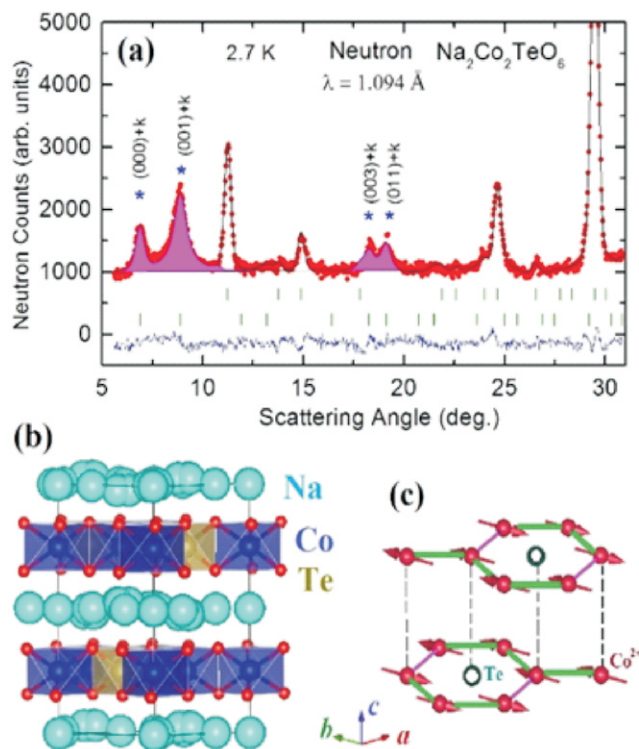


Fig. 2: (a) The Rietveld refined neutron diffraction pattern (shown a limited range for clarity) of $\text{Na}_2\text{Co}_2\text{TeO}_6$ measured at 2.7 K using the PD-1 diffractometer, Dhruva, BARC. The magnetic Bragg peaks are shown by the shaded regions. (b) and (c) The layered crystal and zigzag AFM magnetic structures of $\text{Na}_2\text{Co}_2\text{TeO}_6$, respectively.

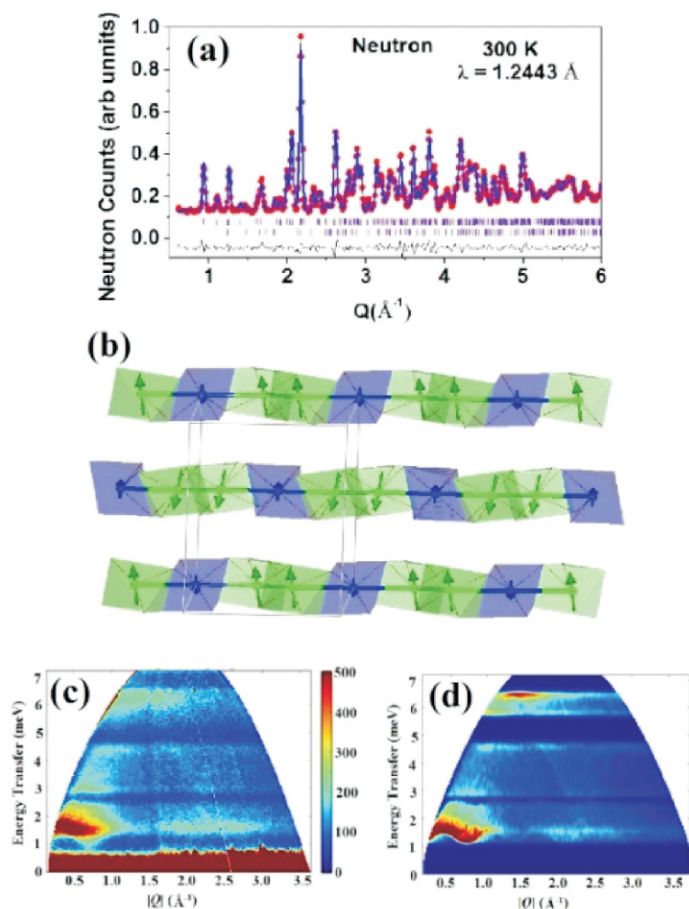


Fig. 3: (a) The Rietveld refined neutron diffraction pattern of $\text{CaNi}_3\text{P}_4\text{O}_{14}$ measured at 300 K using the PD-2 diffractometer, Dhruva, BARC. (b) The spin trimer crystal structure and spin arrangements below the $T_c=16$ K. (c) and (d) The experimentally measured and simulated (by spin wave theory) spin excitation spectra of $\text{CaNi}_3\text{P}_4\text{O}_{14}$.

magnetic Hamiltonian is determined by spin-wave theory analysis of the magnetic excitations, which reveals both ferromagnetic nearest neighbour J_1 and next-nearest neighbour J_2 interactions within the chains, and an antiferromagnetic interchain interaction J_3 . The strengths of the J_1 and J_2 are found to be closer ($J_2/J_1 = 0.81$), and J_3 is determined to be weaker ($|J_3/J_1| = 0.69$) with a weak single-ion anisotropy ($D/J = 0.19$) [5]. The strengths and signs of exchange interactions explain why the 1/3 magnetization is absent in the studied spin-1 compound $\text{CaNi}_3\text{P}_4\text{O}_{14}$ in contrast to its $S=5/2$ counterpart $\text{CaMn}_3\text{P}_4\text{O}_{14}$. Hence, the present study reveals the importance of full knowledge of the exchange interactions in trimer spin-chain compounds to understand their exotic magnetic properties, such as 1/3 magnetization plateau.

Study of phenomenon of magnetization reversal in functional oxides

Magnetization reversal or negative magnetization phenomenon was phenomenologically introduced in spinel ferrites by Néel in 1948 [19, 20]. This phenomenon mainly occurs due to dissimilar magnetization behaviours of two or more magnetic sublattices in materials. We have investigated this technologically important magnetization reversal phenomenon in spinels, garnets, and perovskite compounds by employing microscopic neutron diffraction technique [21-30]. We have given a first microscopic experimental explanation of the magnetization reversal phenomenon [24]. Subsequently, we have written a very first and comprehensive review on the subject covering all physics-related aspects of the phenomenon and its implications in magnetic memory, magneto-caloric and spin resolving devices [21]. Here we report investigations of magnetization reversal phenomenon in rare-earth based NdMnO_3 [22] and $\text{Ho}_3\text{Fe}_5\text{O}_{12}$ [29] magnetic oxides.

Rare-earth ordering driven spin reorientation and magnetization reversal in NdMnO_3

The perovskites are an important class of compounds that show multitude of physical properties such as spin dependent transport, multiferroic behavior, half metallic ferromagnetism, charge, and orbital ordering that are of great importance for various practical

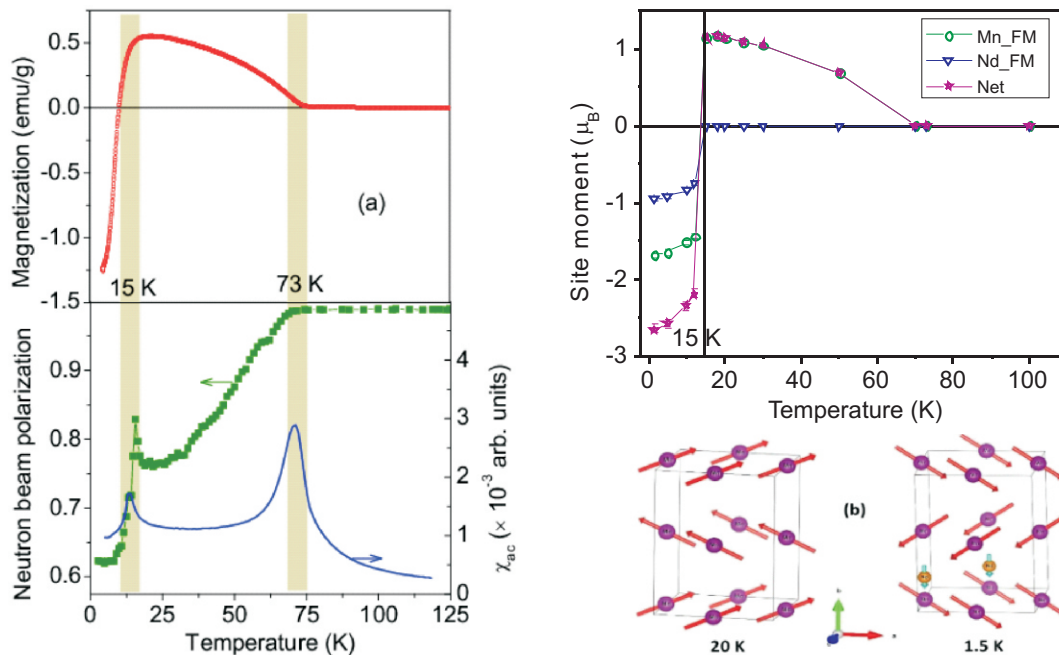


Fig. 4: (a) Magnetic ordering and magnetization reversal in NdMnO₃, shown by dc magnetization under 50 Oe, ac susceptibility (χ_{ac}) at 97 Hz, and neutron depolarization under 10 Oe field. (b) Microscopic understanding of Nd ordering induced Mn spin reorientation and magnetization reversal at 15 K by employing neutron diffraction.

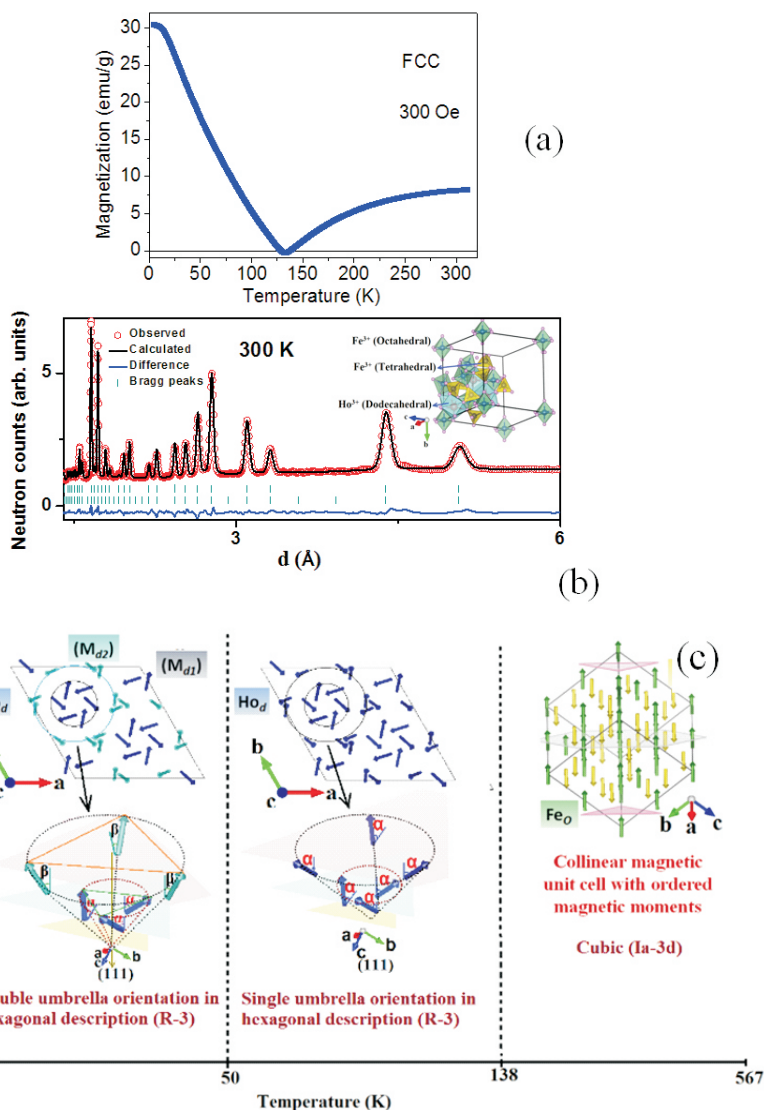


Fig. 5: (a) Magnetization compensation in Ho₂Fe₃O₇ (b) The Rietveld refined neutron diffraction pattern and the derived crystal structure (b) Schematic view of the magnetic unit cell for different temperature regions.

miniaturization and high stability. Here, we report the ionic conduction pathways and its temperature evolution [31-32], by neutron diffraction studies, in some of the magnetic materials that are also useful for the battery or solid oxide fuel cell (SOFC) applications.

Sodium conduction pathways in the layered battery material Na₂Ni₂TeO₆

Na₂Ni₂TeO₆ is layered battery material having Na as an active ion conductor. We have employed neutron diffraction to visualize Na-ion pathways and its temperature evolution in Na₂Ni₂TeO₆. By employing an advanced soft-bond-valence-sum analysis of the neutron diffraction patterns [Fig. 6 (a-b)], we experimentally demonstrate the visualization of microscopic sodium-ion conduction pathways [31] which reveal two-dimensional Na-ion conduction pathways that are confined within the *ab* planes of Na layers [Fig. 6(c-d)].

The experimentally derived pathways are excellent agreement with that recently reported theoretical results of molecular dynamics simulation. Our study further reveals that the layered crystal structure involving Na-ion layers is responsible for high ionic conductivity, and the local crystallographic environment of Na-ion sites is responsible for site-specific conductivity which has a strong temperature dependence [Fig. 6(c-d)].

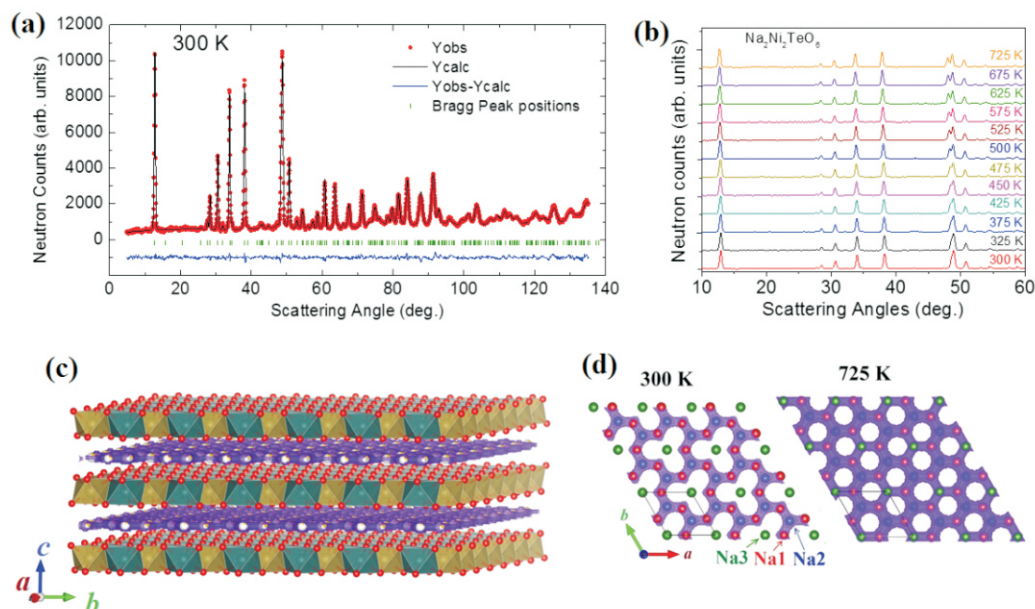


Fig. 6: (a) The Rietveld refined neutron diffraction pattern, measured at 300 K using the PD-2 diffractometer, Dhruva, BARC, for the layered Na-ion battery material $\text{Na}_2\text{Ni}_2\text{TeO}_6$ (b) The temperature dependent neutron diffraction patterns over the temperature range between 300 and 725 K (c) The two-dimensional Na-conduction pathways in the crystal lattice (d) The in-plane view of the Na-ion conduction pathways at 300 and 725 K.

applications. However, the role of rare-earth (R) moment ordering, that introduces finite and anisotropic f - d exchange interactions, in controlling technologically important properties of rare-earth manganites ($RMnO_3$) compounds, is not investigated in great details. In our neutron diffraction study on NdMnO_3 , for the first time, we have observed a strong evidence of rare-earth moment ordering driven Mn spin-reorientation transition in a larger R (Nd) ion based $RMnO_3$ compound. In particular, we show that Nd moment ordering at 15 K derives a Mn spin-reorientation and a concurrent structural distortion in NdMnO_3 compound. Our study also provides a microscopic understanding of the observed magnetic reversal phenomenon (in a field cooled dc magnetization study) [22] at the Nd moment ordering in NdMnO_3 compound.

By employing neutron diffraction, neutron depolarization, dc magnetization and ac susceptibility techniques [Fig. 4(a)], we have revealed a canted antiferromagnetic type spin arrangement (with a net FM component along b axis) for the Mn sublattice in the temperature range of 73 – 15 K. We have also established the ordering of Nd sublattice below 15 K in this compound. For the first time, we have shown that the ordering of the Nd sublattice drives a reorientation (by 180°) of the net FM moment of the Mn sublattice along the b -axis [Fig. 4 (b)]. Such a Mn spin reorientation explains the magnetization reversal phenomenon present in this

perovskite compound [22]. This new finding is significant considering the fact that the $RMnO_3$ compounds with smaller R ions (R : Ho, Er, Yb) show a Mn spin reorientation at rare-earth ordering and depict stronger coupling of the magneto-electric, magneto-elastic, and thermoelectric properties. Our finding, viz. occurrence of Mn spin reorientation in a larger ion (Nd) manganite, should encourage a reinvestigation of the $RMnO_3$ compounds with larger R ions for possible correlations among spin reorientation and magneto-caloric, thermoelectric, dielectric, ferroelectric properties of the $RMnO_3$ compounds.

Magnetization compensation phenomenon and its correlations in $\text{Ho}_3\text{Fe}_5\text{O}_{12}$

The ferrite garnet system, $\text{Ho}_3\text{Fe}_5\text{O}_{12}$ with Fe-Octahedral (Fe_o), Fe-Tetrahedral (Fe_t), and Ho-dodecahedral (Ho_d) magnetic sublattices is another system that exhibits magnetization compensation phenomenon at 138 K (T_{COMP}) [29] as shown in Fig. 5(a). The system exhibits magnetic ordering at 567 K and another magnetic transition at lower temperature (~ 50 K). Macroscopic, mesoscopic, and microscopic understanding of magnetization compensation and magnetic transition at ~ 50 K is studied by dc magnetization, neutron depolarization, and neutron diffraction techniques, respectively. $\text{Ho}_3\text{Fe}_5\text{O}_{12}$ system shows a sign reversal of magnetization below the T_{COMP} under low

(~ 50 Oe) applied magnetic field. Neutron depolarization study infers a zero-domain magnetization state at T_{COMP} with a full recovery of transmitted neutron beam polarization; this confirms the spin compensation at 138 K. Room temperature Rietveld refined neutron diffraction pattern with derived cubic crystal structure is shown in the Fig. 5(b). Our neutron diffraction study has revealed a ferrimagnetic ordering of FeO and FeT sublattices and Hods sublattice ordering takes place below the T_{COMP} into a single umbrella type canted spin configuration. This results in reduction of unit cell symmetry from cubic (1a-3d) to rhombohedral (R-3) [29]. Further below 50 K, Ho^{3+} sites split into two inequivalent magnetic sublattices, having different moments and canting angles, and leading to a double umbrella type magnetic structure as shown in Fig. 5(c).

Ionic conduction pathways in the superionic conductors for SOFC and battery applications

Superionic conductors are an important group of materials that have large-scale technological applications in the areas of energy storage and generation (electrolyzers, batteries, and fuel cells), gas sensors, and electrochromic devices. Such conductors are essential for the development of all-solid-state electrochemical devices, which have many advantages over those based on liquid electrolytes including ease of

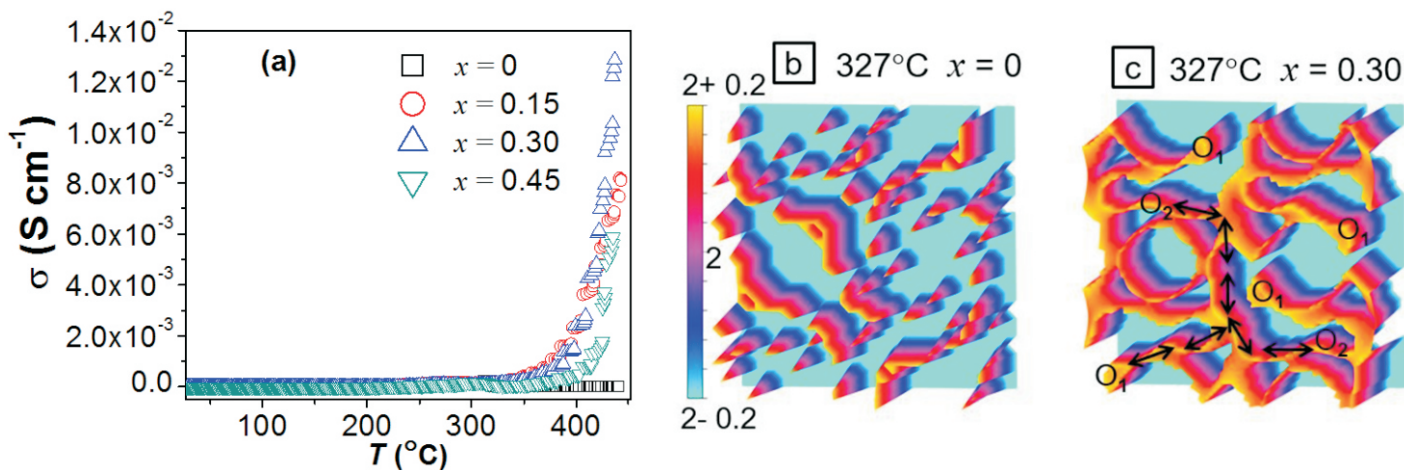


Fig. 7: (a) Temperature variations of ionic conductivities (σ) of $\text{La}_x\text{Y}_{3-x}\text{Fe}_5\text{O}_{12+\delta}$ ($x = 0, 0.15, 0.30$, and 0.45) compounds (b) Discontinuous and (c) continuous oxide ion conduction pathways in (100) plane at 327 °C in the parent ($x = 0$) and La substituted ($x = 0.3$) compounds, respectively.

Neutron investigations of oxide ion conduction pathways in $\text{La}_x\text{Y}_{3-x}\text{Fe}_5\text{O}_{12+\delta}$ garnets

In another study on the La substituted yttrium iron garnets $\text{La}_x\text{Y}_{3-x}\text{Fe}_5\text{O}_{12+\delta}$ ($x = 0 - 0.45$), we address the issue of achieving high oxide ion conductivity [Fig. 7 (a)] at low temperatures (< 500 °C) in stable electrolytes for SOFC technology [32]. The oxide ion conduction pathways have been derived from neutron diffraction data by the soft-bond-valence-sum analysis. We reveal that the oxide ion conduction is based on an excess oxide ion concentration in the garnets and a judicious substitution of high electropositive La^{3+} ions ($x = 0.45$) affords continuous and easy oxide ion conduction pathways through polyhedral networks even at a low temperature of 327°C which are absent in the parent $x=0$ compound [Figs. 7 (b) and (c)]. The observed high oxide-ion conductivity at low temperatures in the present trivalent substituted garnets is a remarkable finding for the development of an efficient SOFC technology.

Summary

In summary, we have presented here structural and magnetic properties of novel functional magnetic materials, investigated by microscopic neutron scattering and other thermodynamic measurements. Microscopic understanding of the relation between the structure and magnetic properties has been obtained using the neutron scattering technique. In some cases, understanding of the relation between the structure (crystal/magnetic) and functionalities at the molecular and

atomic scales has been obtained. The fundamental understanding obtained through neutron scattering study is useful for predictive design of functional materials for memory, energy, and sensors applications of advanced magnetic materials.

Acknowledgment

Authors respectfully acknowledge the contributions of their collaborators in the work reported in this article.

Corresponding Author*

S. M. Yusuf (smyusuf@barc.gov.in)

References

- [1] S. M. Yusuf and A. Kumar, Appl. Phys. Rev. 4, **031303** (2017).
- [2] A. Jain, S. M. Yusuf, P. Kanoo, S. K. Dhar, and T. K. Maji, Phys. Rev. B (rapid) 101, **140** (2020).
- [3] A. K. Bera, S. M. Yusuf, A. Kumar, and C. Ritter, Phys. Rev. B 95, **094424** (2017).
- [4] A. K. Bera, S. M. Yusuf, A. Kumar, M. Majumder, K. Ghoshray and L. Keller, Phys. Rev. B 93, **184409** (2016).
- [5] A. K. Bera, S. M. Yusuf and D. T. Adroja, Phys. Rev. B 97, **224413** (2018).
- [6] A. Yogi, A. K. Bera, A. Mohan, R. Kulkarni, S. M. Yusuf, A. Hoser, A. A. Tsirlin, M. Isobe, and A. Thamizhavel, Inorg. Chem. Frontiers 6, **2736-2746** (2019).
- [7] A. Yogi, A. K. Bera, A. Maurya, R.

Kulkarni, S. M. Yusuf, A. Hoser, A. A. Tsirlin, and A. Thamizhavel, Phys. Rev. B 95, **024401** (2017).

- [8] P. Suresh, K. Vijaya Laxmi, A. K. Bera, S. M. Yusuf, B. Lingam Chittari, J. Jung and P. S. Anil Kumar, Phys. Rev. B 97, **184419** (2018).
- [9] A. Singh, A. Jain, A. Ray, B. Padmanabhan, R. Yadav, V. Nassif, S. Husain, S. M. Yusuf, T. Maitra, V. K. Malik, Phys. Rev. B 96, **144420** (2017).
- [10] R. Shukla, A. Jain, M. Miryala, M. Murakami, K. Ueno, S. M. Yusuf, R. S. Dhaka J. Phys. Chem. C 123, **22457** (2019).
- [11] A. Singh, S. Rajput, P. Balasubramanian, M. Anas, F. Damay, C. M. N. Kumar, G. Eguchi, A. Jain, S. M. Yusuf, T. Maitra, and V. K. Malik, Phys. Rev. B 102, **144432** (2020).
- [12] S. S. Islam, Vikram Singh, K. Somesh, Prashanta K. Mukharjee, A. Jain, S. M. Yusuf, and R. Nath, Phys. Rev. B 102, **134433** (2020).
- [13] K. K. Kumawat, A. Jain, S. S. Meena, and S. M. Yusuf, J. Alloy. Compd., 865, **158849** (2021).
- [14] P. W. Anderson, Science 235, **1196** (1987).
- [15] P. Kanoo, C. Madhu, G. Mostafa, T. K. Maji, A. Sundaresan, S. K. Pati and C. N. R. Rao, Dalton Trans. **5062-5064** (2009).
- [16] S. H. Chun, et al., Nat. Phys. 11, **462** (2015).

- [17] A. Banerjee et al., Nat. Mat. 15, **733** (2016).
- [18] H Liu and G. Khaliullin, Phys. Rev. B 97, **014407** (2018).
- [19] L. Neel, Ann. Phys. (Paris) 3, **137** (1948)
- [20] T. Nagata, Rock Magnetism, second ed., Maruzen, Tokyo, 1961.
- [21] A. Kumar and S.M. Yusuf, Phys. Rep. 556, **1** (2015).
- [22] A. Kumar, S. M. Yusuf, and C. Ritter, Phys. Rev. B 96, **014427** (2017).
- [23] A. Kumar, S. M. Yusuf, J. Appl. Phys. 121, **223903** (2017).
- [24] A. Kumar, S. M. Yusuf, L. Keller, JV Yakhmi, Phys. Rev. Lett. 101, **207206** (2008).
- [25] A. Kumar and S. M. Yusuf, Physica B 551, **104** (2018).
- [26] M.Ghanathe, A. Kumar, and S. M. Yusuf, J. Appl. Phys. 125, **093903** (2019).
- [27] Deepak, A. Kumar, and S.M. Yusuf, J. App. Phys. 127, **213903** (2020).
- [28] M. Y. Yang, S.Seong, E. Lee, M.Ghanathe, A. Kumar, S. M. Yusuf, Y. Kim, J. S. Kang Appl. Phys. Lett. 116, **252401** (2020).
- [29] M. Ghanathe, A. Kumar, I. da Silva, and S. M. Yusuf, J. Magn. Magn. Mater. 523, **167632** (2021).
- [30] A. Kumar, S. K. Giri, T. K. Nath, C. Ritter, S. M. Yusuf, J. Appl. Phys. 128, **203901** (2020).
- [31] A. K. Bera and S. M. Yusuf, J. Phys. Chem. C, 124, **4421** (2020).
- [32] D. R. Bhosale, S. M. Yusuf, A. Kumar, M. D.Mukadam, S. I. Patil, Phys. Rev. Mater. 1, **015001** (2017).